Industrial Crops & Products 113 (2018) 64–74

Contents lists available at ScienceDirect

Industrial Crops & Products

journal homepage: www.elsevier.com/locate/indcrop

Structural and compositional changes in sugarcane bagasse subjected to hydrothermal and organosolv pretreatments and their impacts on enzymatic hydrolysis

Melissa Espirito Santo[a], Camila A. Rezende[b], Oigres D. Bernardinelli[a], Nei Pereira Jr.[c], Antonio A.S. Curvelo[d], Eduardo R. deAzevedo[a], Franscisco E.G. Guimarães[a], Igor Polikarpov[a,*]

[a] Department of Physics and Interdisciplinary Science, São Carlos Institute of Physics, University of São Paulo, Av. Trabalhador São-carlense, 400, São Carlos, SP, 13566-590, Brazil
[b] Institute of Chemistry, University of Campinas, P.O. Box 6154, Campinas, SP, 13083-970, Brazil
[c] Biochemical Engineering Department, School of Chemistry, Federal University of Rio de Janeiro (UFRJ), Block E, Room 121, Ilha do Fundão, 21949-900, Rio de Janeiro, RJ, Brazil
[d] Department of Physical-Chemistry, Institute of Chemistry of São Carlos, University of São Paulo, Av. Trabalhador Sãocarlense, 400, São Carlos, SP, 13566-590, Brazil

ARTICLE INFO

Keywords:
Sugarcane bagasse
Enzymatic hydrolysis
Bioethanol
Pretreatments
Biophysical investigations

ABSTRACT

Economical sustainability of cellulosic ethanol technology still requires considerable improvements in efficacies of both pretreatment and enzymatic hydrolysis steps. In this work a number of physical techniques were applied to characterize sugarcane bagasse samples that underwent hydrothermal and/or organosolv pretreatments under variable conditions and to correlated the observed changes with the efficiency of enzymatic hydrolysis. Confocal and field emission scanning electron microscopy studies revealed morphological changes in lignin distribution in the plant cell wall. The hydrothermal pretreatment caused a disorder in the arrangement of the lignin, whereas organosolv pretreatment partially removed lignin from bagasse and fraction of it redeposited at the surfaces of cellulose fibers. The delignification process was also analyzed by both chemical composition analysis and nuclear magnetic resonance. Pretreatment conditions leading to a significant increase of the efficiency of enzymatic hydrolysis were identified. Our studies open avenues for further biophysical investigations of pretreated lignocellulosic biomass, which could lead to its improved enzymatic hydrolysis.

1. Introduction

Dwindling reserves of fossil fuels and growing concerns about greenhouse gas emissions and environmental impacts are increasingly encouraging the use of renewable resources and the development of alternative feedstocks for biofuel production worldwide. In Brazil, bioethanol production is still largely based on sugarcane juice fermentation. However, sugarcane bagasse, which is the residue from the milling process, is an energy-rich structure, containing cellulose, hemicelluloses and lignin (Soccol et al., 2010). The use of agricultural residues from the first-generation ethanol production, such as sugarcane bagasse and leaves, can contribute to the complete utilization of the raw material in the integrated biorefineries (Dias et al., 2012). Processing of lignocellulosic feedstock to ethanol usually involves four major unit operations: pretreatment, hydrolysis, fermentation, and distillation (Taherzadeh and Karimi, 2007), but these processes are still not fully efficient and should be optimized.

The sugarcane bagasse is mainly composed of tridimensional structural networks of cellulose intertwined by hemicelluloses and lignin (Rezende et al., 2011). Lignin is a phenolic, branched, and hydrophobic structure, highly resistant to degradation, that unproductively adsorbs enzymes and hinders cellulose accessibility during enzymatic hydrolysis of biomass (Achyuthan et al., 2010; Zhang and Lynd, 2004). Therefore, lignin content and distribution are recognized as important factors determining cell wall recalcitrance to enzymatic depolymerization (Paul, 2014). Because of this, different pretreatments are normally applied prior to enzymatic hydrolysis step in order to unstructure the cell walls and to partially remove hemicellulose and lignin. Pretreatments provide fractionation of lignocellulosic biomass, thus decreasing its recalcitrance and resulting in better yields of monomeric fermentable sugars released by the enzymatic hydrolysis step (Himmel et al., 2007; Kumar et al., 2009; Taherzadeh and Karimi, 2007). Currently, enzymatic hydrolysis is the most widely used method for bioethanol production, since it is a specific and environmentally

* Corresponding author.
E-mail address: ipolikarpov@ifsc.usp.br (I. Polikarpov).

https://doi.org/10.1016/j.indcrop.2018.01.014
Received 1 October 2017; Received in revised form 12 December 2017; Accepted 8 January 2018

friendly process, that can be run at low temperatures and does not produce by-products that may inhibit the subsequent fermentation step (Himmel et al., 2007; Sheehan and Himmel, 1999; Wingren et al., 2005). On the other hand, enzymes are expensive and contribute to the relatively high costs of the second-generation ethanol.

A choice of a particular pretreatment is important, because different pretreatments have different mechanisms of action that will affect the cell wall structure, the chemical species to be released and the inhibitory co-products to be generated (Himmel et al., 2007; Kumar et al., 2009; Soccol et al., 2010). Organosolv pretreatment efficiently removes lignin from the lignocellulosic materials through the partial hydrolysis of lignin bonds. It decreases the lignin content in the cell wall by breaking α-aryl ether and arylglycerol-β-aryl ether (β−O−4) bonds of lignin macromolecule (Nakagame et al., 2011; Sarkanen et al., 1981), imparting significant changes in the lignin structure, including increases in phenolic groups, and decreases the average molecular weight of the lignin (Gilarranz et al., 2000). This pretreatment could be more expensive than some others pretreatment processes, but can provide lignin-derived value-added products that might contribute to the economical viability of organosolv pretreatment in the context of the integrated biorefineries. Hydrothermal treatment has lower costs and reduced environmental impacts (Brodeur et al., 2011; Ma et al., 2014). This pretreatment only utilizes water at high temperatures, which mainly results in hemicelluloses solubilization and structural modifications of the biomass that lead to enhanced enzymatic hydrolysis. Hydrothermal pretreatment temperatures (typically ranging from 160 °C to 240 °C) and the biomass residence time will determine the types and the amount of sugars being released from the biomass (Yu et al., 2010). Hydrothermal pretreatment relies on autohydrolysis, which makes use of acetic acid liberated from hemicellulose's acetyl groups to catalyze the breakdown of polysaccharides into shorter chain oligosaccharides and simple sugars (Roos et al., 2009; Tunc and Van Heiningen, 2011). The hydrothermal pretreatment of lignocellulosic materials involves mostly solubilization of hemicelluloses, and also extractives, sugars and small fragments of lignin (Vázquez et al., 2005; Xing et al., 2011).

In this study the effects of two different pretreatments (organosolv and hydrothermal), applied independently and/or sequentially, to the sugarcane bagasse samples were analysed, aiming to find conditions and pretreatment combinations that lead to more efficient enzymatic hydrolysis. A comprehensive set of physical techniques combined with chemical composition analyses was applied to reveal the chemical and structural changes induced by the pretreatments in the sugarcane bagasse and their impacts on the efficiency of enzymatic hydrolysis. Insights into untreated and preteated biomass structure and composition, combined with the experimentally measured enzymatic hydrolysis yields, provide a unique opportunity for better comprehension of the impact of pretreatment-induced changes taking place in sugarcane bagasse samples on efficiencies of their enzymatic hydrolysis.

2. Material and methods

2.1. Material

Sugarcane bagasse from the last milling step for juice extraction was provided by the Cosan Group (Usina da Serra/Ibaté, São Paulo, Brazil). This material was milled using knife mill and rinsed with hot water (50 °C). Next, bagasse was dried in the oven at 60 °C for 24 h. Prior to each experiment, the moisture content was measured using an analytical balance (Shimadzu; Kyoto, Japan). All the analyses and measurements described in this work were performed with the same batch of samples.

2.2. Bagasse pretreatments

Sugarcane bagasse was pretreated using both hydrothermal and organosolv pretreatments. These pretreatments were applied separately and/or combined under different conditions. Hydrothermal pretreatment was applied using hot water as a reaction media in four distinct reaction times: 1 min (Hyd_1′), 30 min (Hyd_30′), 45 min (Hyd_45′) and 60 min (Hyd_60′) at 160 °C in a reactor (AU/E-20 model, Regmed). The pressure was kept at 7 bar and a 1:10 solid to liquid ratio (grams of bagasse/mL of water) was used. According to previous works, the temperature of 160 °C is close to the optimal for the sugarcane bagasse pretreatment (Yu et al., 2013), whereas at higher temperatures and more severe conditions, xylose and glucose degradation products were produced at significantly highier levels. Here, four distinct reaction times were applied to explore this particular temperature condition of the hydrothermal methodology.

In the case of organosolv pretreatments, previous studies also showed that they represent a potential method for delignification of plant biomass that simultaneously preserves the cellulose fraction (Novo et al., 2011). Novo and collaborators showed that one of the best pretreatment conditions for lignin removal by the organosolv method could be achieved at 190 °C. Furthermore, different reaction times have been applied and 150 min was found to be an efficient condition (Novo et al., 2011). In the present work, the study of shorter times were included to verify if they could be enough to introduce significant changes in the sugarcane bagasse structure. Thus the organosolv treatement was carried out in ethanol/water solutions (50% v/v) heated at 190 °C in a glycerin bath for three different reaction times: 50 min (Org_50′); 100 min (Org_100′) and 150 min (Org_150′).

Finally, the combined action of both hydrothermal and organolsolv pretreatments applied in sequence to increase the efficiency of enzymatic hydrolysis was also evaluated. Combined treatments consisted of a first hydrothermal step for 30 min or 60 min at 160 °C, followed by an organosolv step at 190 °C (Hyd_30′ + Org_50′; Hyd_30′ + Org_100′; Hyd_30′ + Org_150′; Hyd_60′ + Org_50′; Hyd_60′ + Org_100′; Hyd_60′ + Org_150′). After each pretreatment step the liquors were separated from the solid fractions by filtration, these were firstly rinsed with ethanol and then with tap water until reaching a neutral pH. The solids were dried in oven for 24 h at 60 °C and stored for characterization of its chemical composition and physical structure.

2.3. Chemical composition determination

The chemical composition for untreated and pretreated sugarcane bagasse solids was obtained following the protocol established by Rocha and coworkers (2011), with some modifications (Rezende et al., 2011). Initially, the solid samples were grounded using a knife mill, prior to passing through a 20-mesh sieve and had their dry matter weight determined. Extractives were removed from the untreated bagasse, using a 1:1 cyclohexane/ethanol solvent mixture under reflux in a Soxhlet apparatus for *ca.* 8 h, followed by water extraction for 5 cycles with 8 h each. Fiber extraction with cyclohexane-ethanol allows removal of waxes, lipids and tannins from the fiber surface and therefore has been applied (Park et al., 2008; Vallejos et al., 2012). After extraction, samples were dried and the content of extractives was determined.

Solid biomass samples (2 g) were hydrolyzed using 15 mL of a 72% H2SO4 solution at 45 °C, under constant stirring for 7 min. Then, 275 mL of distilled water were added to this mixture and the material was kept at 120 °C for 30 min. The remaining solids were separated from the reaction liquors by filtration in filter paper. The solid fraction was rinsed until a neutral pH was reached and then oven dried at 105 °C to a constant weight. This fraction corresponded to the biomass insoluble lignin and ashes. By calcination of this solid in a muffle furnace at 800 °C for 2 h, the ash (remaining inorganic fraction) and the lignin (calcinated fraction) amounts were determined. The acid soluble lignin was determined in the reaction liquor by UV-VIS, as previously described (Rocha et al., 2011). The composition of hydrolysate liquors including soluble sugars, organic acids and hydroxymethylfurfural was

determined by HPAE-PAD (High Performance anion-exchange chromatography with pulsed amperometric detection), after neutralization of the liquor with a 2 M barium hydroxide solution. The equipment used for HPAE-PAD analysis (Dionex ICS 5000, ThermoFisher, Sunnyvale, CA, USA) was equipped with a CarboPac PA1 column (ThermoFisher) and a 400 mM NaOH solution was used as mobile phase (flow rate 1 mL/min) in a multistep process (10–400 mM). The cellulose fraction was obtained accounting for the amounts of glucose, cellobiose and hydroxymethylfurfural, while the hemicelluloses fraction was calculated by taking into account the amounts of xylose, fucose, rhamnose, arabinose, galactose, furfural, galacturonic and glucuronic acids. All these components were quantified in duplicate, using commercial standards, and expressed as an average (± standard deviation). Prior to injection, samples were filtered using a Sep-Pak C18 filter (Waters – Milfords, MA, USA) for lignin removal. The HPAE-PAD was also used for monomeric sugars content analysis in liquors generated by enzymatic hydrolysis.

2.4. ^{13}C solid-state nuclear resonance magnetic (^{13}C ssNMR)

The data were collected using a Varian Inova Spectrometer (Varian, Palo Alto, CA, USA) operating in frequencies of 100.5 MHz and 400.0 MHz for ^{13}C and ^{1}H, respectively. A Jackobsen probe 7 mm double resonance with sample rotation pneumatic system built around the magic angle spinning probe with a frequency stability superior to 2 Hz was used for data collection. The CPMASTOSS pulse sequence (ramped cross-polarization under magic angle spinning and total suppression of spinning sidebands) allows integration of excitation by cross-polarization (CP) between the ^{1}H and ^{13}C nuclei with a radio-frequency ramp, sample rotation around the magic angle (MAS: magic angle spinning), elimination of sidebands (TOSS: total suppression of spinning sidebands) and heteronuclear uncoupling of the ^{1}H channel, which resulted in the acquisition of a high resolution ^{13}C ssNMR spectrum. All ^{13}C ssNMR experiments were carried out as described in the literature (Rezende et al., 2011). The MAS frequency was 6 kHz and 90° pulse lengths were 4.5 and 4.0 μs, for ^{13}C and ^{1}H, respectively. Cross polarization was achieved with ramped RF amplitude (80–100%) using a contact time of 1 ms. Time proportional phase modulated (TPPM) heteronuclear decoupling was performed with a decoupling frequency of 60 kHz. All ^{13}C ssNMR measurements were performed using 5 s recycle delays.

2.5. Field emission scanning electron microscopy (FESEM)

Morphology of the sugarcane bagasse samples before and after the pretreatments was analyzed by FESEM. Dried samples were fixed in suitable stubs with carbon tape and then coated with Au in a SCD 050 sputter coater (Oerlikon-Balzers, Balzers, Liechtenstein). Secondary electron images were obtained using a scanning electron microscope equipped with a field emission gun (FESEM – FEI Quanta 650). Analyses of the samples were performed under vacuum, using a 5 kV acceleration voltage and a large number of images were obtained at different areas of each sample (20–25 images per sample) to guarantee the reproducibility of the results.

2.6. Enzymatic hydrolysis

Enzymatic hydrolysis assays were carried out with untreated and pretreated sugarcane bagasse samples, using a substrate at 4% (w/V) concentration in 50 mM sodium citrate buffer (pH 5.0). Flasks were incubated in an orbital shaker at constant agitation (150 rpm) and temperature (50 °C). The enzymatic blend consisted of 10 filter paper units (FPU) of Accellerase 1500 (Genencor, Rochester, NY, USA) mixed with 15 Beta-Glucanase Units (BGU) of Novozyme 188 (Novozymes, Bagsvaerd, Denmark) per gram of biomass. The soluble hydrolysate products were analyzed by HPAE-PAD, as described in chemical composition determination for hydrolysate liquors. The cellulose hydrolysis yield (HY) was determined considering the amount of released glucose and the fraction of cellulose in a particular bagasse sample, as previously described (Maeda et al., 2011). Hydrolysis yields were also calculated for these samples, as the mass ratio between the glucose amount released by enzymatic hydrolysis in a specific sample and the cellulose amount in this sample (termed as enzymatic hydrolysis yield) or the cellulose amount in the original untreated biomass (total saccharification yield). Since pretreatments generally lead to a partial loss of glucans, a total saccharificcation yield tends to be smaller than an enzymatic hydrolysis yield for a particular pretreatment.

2.7. X-Ray diffraction

X-Ray diffraction data were collected on a diffratometer Rotaflex RU200 B (Rigaku Tokyo, Japan) using monochromatic radiation from a copper rotating anode (1.5418 Å) operating at 45 kV and 36 mA and equipped with a graphite monochromer, according to a previous work (Rezende et al., 2011)

2.8. Confocal microscopy and FLIM

Confocal laser scanning microscopy (CLSM) was used to map lignin distribution in the samples and to obtain information on its molecular arrangement within the cell wall, by measuring lignin fluorescence emitting spectra and its fluorescence decay times. Pretreated and untreated bagasse samples were suspended in water and dropped on the coverslides. CLSM images were obtained as an average of three scans, using a Plan-Apochromat objective lens (20x, water immersion) and a Zeiss LSM 780 confocal microscope with a Coherent Chameleon laser (Tisapphire) as a source for two-photons (2 P) excitation experiments. The total number of dots per image was 1024 × 1024 and the area of each pixel was associated with the optical resolution of the lens resulting in a lateral resolution of about 300 nm. CLSM were collected from the surface of the samples. For FLIM analysis, the 2P laser was pulsed at 80 MHz with a time response limited to about 100 ps at 800 nm and an average power of 15 mW.

3. Results and discussion

3.1. Pretreatment and chemical characterization

The content of the main components of bagasse samples before and after the pretreatments are given in Table 1. Table 1 shows that the hydrothermal pretreatments at 160 °C at all the reaction times (from 1 to 60 min) have little effect on the lignin fraction of the bagasse samples. Its concentration was approximately constant under the applied conditions of hydrothermal pretreatment. There was, however, a moderate solubilization of hemicellulose (a maximum decrease of *ca.* 3.8% in the total amount of hemicelluloses) under longer pretreatment times (45 and 60 min). However, noticeable cellulose enrichment could be observed, particularly at longer pretreatments, probably due to the solubilization of the extractives and also hemicelluloses, and decrease in ashes content.

Organosolv pretreatments, on the other hand, partially hydrolyze lignin and lignin–carbohydrate bonds, resulting in a more efficient removal of both lignin and hemicelluloses (Nakagame et al., 2011). These effects may explain an observed increase in solubilization of lignin under the organosolv pretreatment at 190 °C at different reaction times, and especially for the samples treated for 100 min, as well as reduced percentages of both lignin and hemicelluloses in the corresponding pretreated biomass samples (Table 1). The cellulose fraction increases proportionally in the samples as the amount of other cell wall components decrease.

The combined Hyd_30′ + Org_50′, Hyd_30′ + Org_100′, Hyd_60′ + Org_50′, Hyd_60′ + Org_100′ pretreatments resulted in

Table 1
Chemical composition of sugarcane bagasse before and after pretreatments.

	Composition (%)					Concentration (mg/mL)		
Pretreatments	Celullose	Hemicellulose	Lignin	Ash	Total	Cellulose	Hemicellulose	Lignin
Untreated	38.3 ± 0.1	20.1 ± 0.1	29.0 ± 1.0	6.0 ± 0.3	100.4* ± 1.9	383 ± 1	201 ± 1	290 ± 1
Hyd_1′	41.5 ± 0.5	18.8 ± 0.1	28.8 ± 1.0	4.5 ± 0.3	93.6 ± 1.9	332 ± 5	150 ± 1	230 ± 1
Hyd_30′	46.5 ± 0.3	19.3 ± 0.1	27.8 ± 3.0	4.0 ± 1.8	97.6 ± 5.2	285 ± 3	132 ± 1	191 ± 3
Hyd_45′	50.0 ± 4.0	16.3 ± 0.1	28.3 ± 0.2	5.5 ± 0.1	100.1 ± 4.4	266 ± 40	105 ± 1	181 ± 2
Hyd_60′	57.0 ± 0.3	16.8 ± 0.2	28.2 ± 0.8	3.7 ± 0.5	105.7 ± 1.8	258 ± 3	105 ± 2	175 ± 8
Org_50′	55.3 ± 8.0	14.9 ± 3.1	21.8 ± 2.0	4.6 ± 0.1	96.6 ± 13.2	254 ± 80	91 ± 31	134 ± 20
Org_100′	65.6 ± 5.9	7.9 ± 0.1	18.5 ± 0.1	5.3 ± 0.1	97.3 ± 6.2	203 ± 59	38 ± 1	91 ± 1
Org _150′	69.3 ± 4.3	9.1 ± 0.1	14.6 ± 0.1	5.7 ± 0.2	98.7 ± 4.7	195 ± 43	42 ± 1	43 ± 1
Hyd_30′+ Org_50′	64.8 ± 7.7	9.7 ± 0.1	21.2 ± 0.1	4.2 ± 0.1	99.9 ± 8.0	228 ± 77	53 ± 1	53 ± 1
Hyd_30′+Org_100′	66.3 ± 8.7	10.5 ± 0.1	15.7 ± 0.2	5.6 ± 0.1	98.1 ± 9.1	204 ± 87	52 ± 1	52 ± 2
Hyd_30′+Org_150′	79.2 ± 0.5	5.2 ± 0.1	10.9 ± 0.2	6.0 ± 0.3	101.3 ± 1.1	187 ± 5	24 ± 1	23 ± 2
Hyd_60′+ Org_50′	64.4 ± 5.0	10.6 ± 0.1	16.7 ± 0.3	5.2 ± 0.2	96.9 ± 5.6	207 ± 50	53 ± 1	53 ± 3
Hyd_60′+Org_100′	63.7 ± 0.9	6.8 ± 0.1	18.9 ± 0.1	5.0 ± 2.0	94.4 ± 3.1	197 ± 9	32 ± 1	32 ± 1
Hyd_60′+Org_150′	76.4 ± 2.1	7.4 ± 0.1	13.0 ± 0.5	5.3 ± 0.1	102.1 ± 2.8	182 ± 21	32 ± 1	32 ± 5

*The extractives percentage detected for the *untreated* sample was 7.0 ± 0.4

lignin and hemicelluloses removal comparable to those obtained in the organosolv pretreatments Org_100′ and Org_150′ in a single step. Thus, pretreatments that combine hydrothermal pretreatment step and organosolv pretreatment with shorter residence times (of 50 min and 100 min) do not seem to be more efficient in lignin and hemicellulose removal as compared with a single organosolv pretreatment for 100 min or 150 min. Under these conditions, a single-step organosolv pretreatment could be more effective.

The two pretreatment combinations that stand out in terms of lignin and hemicelluloses solubilization are the combined Hyd_30′ + Org_150′ and Hyd_60′ + Org_150′ pretreatments. Under these conditions, the lignin concentrations were considerably decreased from 29.0% in the untreated bagasse to 10.9 and 13.0%, respectively, in the pretreated samples. As a result of lignin and hemicelluloses removal, the cellulose content of the pretreated samples was enriched, with the cellulose concentrations increasing from 38% in the untreated sample to 79% and 76%, respectively (Table 1).

In order to better evaluate these results and their effects on the sample morphology, the physical analyses focused on lignin detection were useful. As a first approach ^{13}C solid-state nuclear magnetic resonance (^{13}C ssNMR) technique was applied, which allowed a detailed analysis of the biomass samples. CPMASTOSS ^{13}C ssNMR spectra of the sugarcane bagasse samples that underwent different pretreatments are shown in Fig. 1. Chemical displacements were attributed as described previously (Rezende et al., 2011; Templeton et al., 2010; Wickholm et al., 1998).

The peaks between 50 and 120 ppm are typical for cellulose carbons, but this region also shows peaks of hemicelluloses and lignin (Fig. 1). The peaks between 3 (62.6 ppm) and 7 (84 ppm) are characteristic of carbons C6 from the cellulose amorphous fraction, while peaks 4 (65.0 ppm) and 8 (88.9 ppm) are typical of carbons C6 and C4 from the crystalline fraction of the cellulose (Hallac et al., 2009; Hu et al., 2011; Sannigrahi et al., 2010). Lignin peaks are distributed throughout the spectral region including 2, 11, 12, 13, 14, 15 and 16 (peaks exclusively assigned to lignin). Hemicelluloses peaks are also widely distributed throughout the spectral region, with hemicelluloses carbon peaks contributions identified as 1, 3, 6, 7, 9 and 17 (Kartal et al., 2007; Rezende et al., 2011; Templeton et al., 2010; Wickholm et al., 1998)

The ^{13}C ssNMR spectra of the samples hydrothermally pretreated for different periods of times are very similar to the ^{13}C ssNMR spectrum obtained for the untreated sample (Fig. 1A). In line with the previous studies (Rezende et al., 2011), this suggests that these pretreatments do not promote an efficient removal of lignin, just as indicated by our chromatography analyses of the same samples (Table 1). In contrast, the samples pretreated with organic solvent (ethanol 50%) for 50 min, showed a reduction in hemicelluloses, as can be noticed in peaks 1, 9, 15 and 17, as well as in peaks 2, 11, 12, 13, 14 and 16 (Fig. 1B). After 100 min of organosolv pretreatment, the hemicellulose signals turn virtually undetectable in the ^{13}C ssNMR spectra and the lignin signal drastically reduces. These results corroborate with chromatography analyses (Table 1) that showed a decrease of hemicelluloses concentration from 20.1% to 7.9% and of lignin concentration from 29.0% to 18.5% in comparison with the untreated *in natura* sample. Therefore it is possible to conclude that the organosolv pretreatment applied for 100 min is sufficient for an effective removal of both, hemicelluloses and lignin from the sugarcane bagasse samples.

^{13}C ssNMR spectra of the samples that underwent the combined hydrothermal-organosolv pretreatments showed efficient removal of both hemicelluloses and lignin (Fig. 1C–D). The reduction in the intensity of signals 1 and 17 indicates a decrease in the hemicelluloses content in the pretreated sample. Furthermore, lignin signals (2, 11, 12, 13, 14, 15 and 16) also decreased, thus suggesting that lignin was also removed by the combined pretreatment. All these results are consistent with our chromatography analyses that showed that the best result to improve the cellulose content was achieved under Hyd_30′ + Org_150′ pretreatment that decreased hemicellulose content from 20.1% to 5.2% and the lignin fraction from 29.0% to 10.9% in comparison with unpretreated samples (Table 1).

3.2. Structural and morphological analysis

Changes in crystallinity are often associated with the modifications in the cellulose structure after biological, physical and chemical pretreatments. Due to the strong conformational dependence of the ^{13}C ssNMR spectra, the signals arising from the more ordered internal (crystalline) and the ones from the more disordered (amorphous) and external cellulose chains can be easily dintinguished. This allows the calculation of a ^{13}C ssNMR-based crystallinity index (ssNMR-CI), which is estimated by dividing the integrated intensity associated to the 88 ppm (assigned to C4 from the more ordered internal cellulose chains) signal by the total integrated intensity of the signal corresponding to the C4 carbons (Park et al., 2010; Pu et al., 2006; Sannigrahi et al., 2010). To evaluate the signals C4 signals were deconvoluted, using Gaussian and Lorentzian lines, as reported by Park et al. (2010). The important difference between the ssNMR-CI and the CI calculated by XRD (XRD-CI) is that, the first index is mostly associated to the crystallinity of cellulose as compared to the cellulose amorphous fraction of the biomass (Bernardinelli et al., 2015), while the latter index compares the diffraction intensities from the crystalline cellulose with the scattering from the total amorphous fraction of the biomass (including also lignin and hemicelluloses). The CIs of each

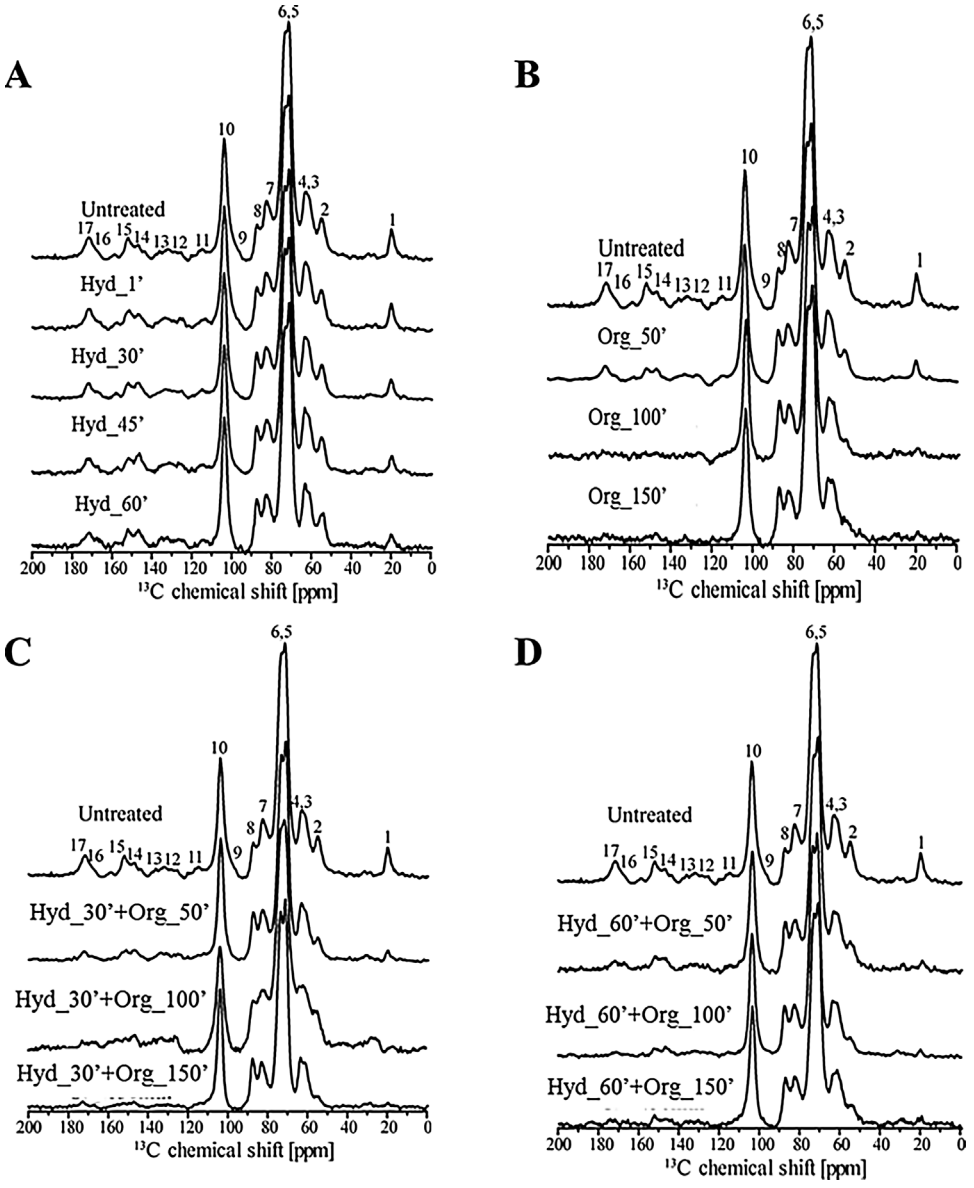

Fig. 1. CPMASTOSS spectra of sugarcane bagasse. (A) The ssNMR spectra obtained from the samples hydrothermally pretreated under different residence times and from the samples in unpretreated control group. (B) The ssNMR spectra of Org_50′; Org_100′ and Org_150′ compared to the untreated sample. (C) Hyd_30′ + Org_50′; Hyd_30′ + Org_100′; Hyd_30′ + Org_150′. (D) ssNMR spectra from Hyd_60′ + Org_50′; Hyd_60′ + Org_100′; Hyd_60′ + Org_150′.

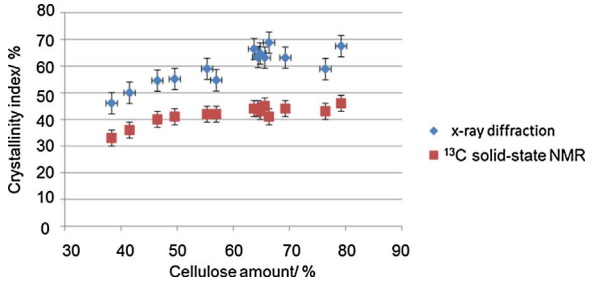

Fig. 2. Cellulose crystallinity indices calculated from ^{13}C solid-state NMR and X-ray diffraction data for untreated sugarcane bagasse samples and the samples after hydrothermal (1, 30, 45 and 60 min), organosolv (50, 100 and 150 min) and combination of hydrothermal (30 and 60 min) with organosolv (50, 100 and 150 min) pretreatments.

sample obtained by these two different techniques were calculated in this work and compared with each other (Fig. 2 and Table 2).

The crystallinity indices obtained by ssNMR and XRD techniques follow a similar rising trend (Fig. 2). However, the absolute value of the CI obtained by X-ray is consistently higher than the one obtained by ssNMR. This might be explained by the fact that the simplified method

Table 2
Crystallinity index measured by x-ray diffraction and solid state nuclear magnetic resonance.

	Crystallinity index (CI)/%	
Pretreatments	x-ray diffraction	^{13}C ssNMR
Untreated	46 ± 4	33 ± 3
Hyd_1′	50 ± 3	35 ± 2
Hyd_30′	55 ± 2	40 ± 2
Hyd_45′	55 ± 1	41 ± 1
Hyd_60′	55 ± 3	41 ± 2
Org_50′	59 ± 2	42 ± 1
Org_100′	63 ± 2	37 ± 1
Org _150′	67 ± 1	45 ± 1
Hyd_30′+ Org_50′	65 ± 2	43 ± 1
Hyd_30′+ Org_100′	69 ± 1	48 ± 1
Hyd_30′+ Org _150′	67 ± 1	45 ± 1
Hyd_60′+ Org_50′	63 ± 2	45 ± 2
Hyd_60′+ Org_100′	66 ± 1	43 ± 1
Hyd_60′+ Org _150′	59 ± 2	43 ± 2

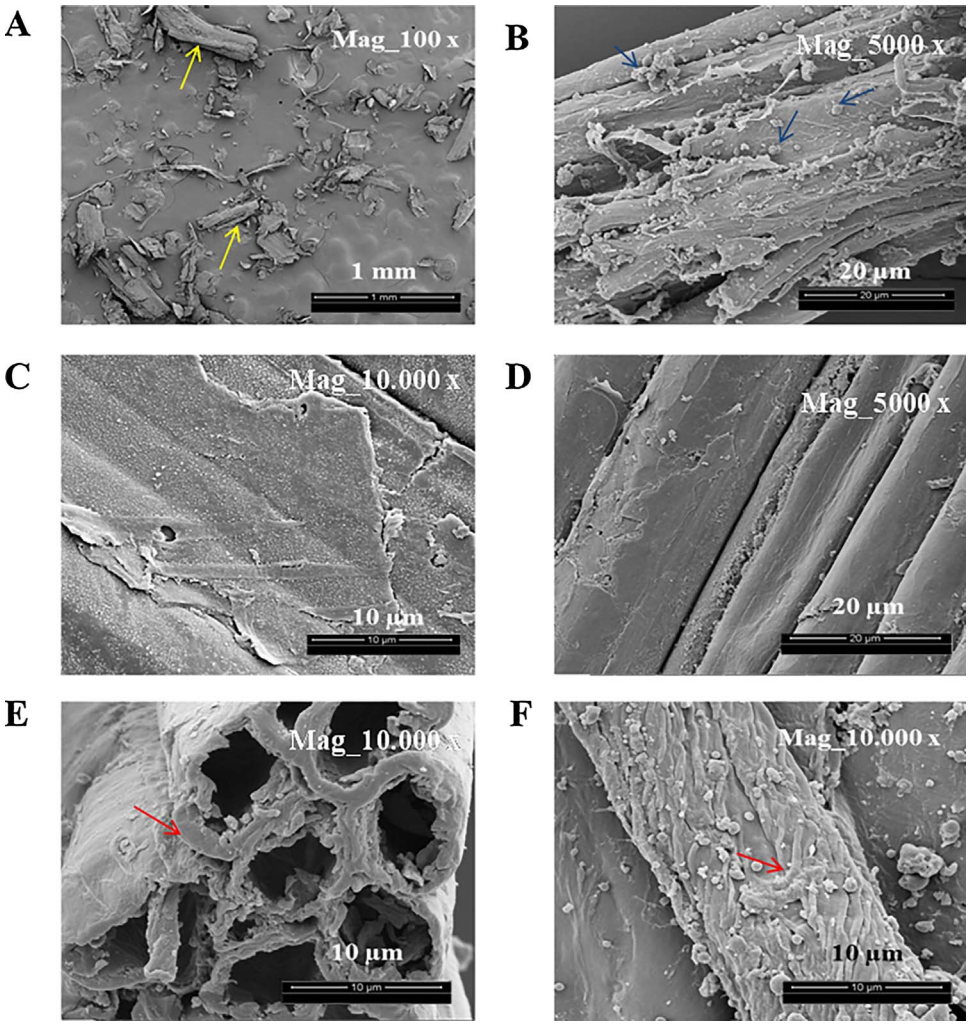

Fig. 3. Field emission scanning electron microscopy (FESEM) images of the bagasse samples before and after pretreatments. (A) A general view of the untreated bagasse, showing fibers (yellow arrows) and particulate material (white arrows). Sugarcane bagasse fibers after pretreatments (B) Hyd_60′ + Org_150′. (C) Hyd_1′. (D) Hyd_60′. (E) Hyd_60′, showing a cross section of the fiber bundle, with the fiber on the surface of the bundle becoming more detached from the others (green arrow). (F) Hyd_60′ + Org_150′, showing a more advanced stage of unstructuring and lignin redeposition (red arrow). (For interpretation of the references to colour in this figure legend, the reader is referred to the web version of this article.)

of CI calculation based on the X-ray diffractogram evaluation overestimates the amount of CI (Lima et al., 2014; Park et al., 2010). This occurs essentially because CI is calculated from the height ratio between the apparent intensity of the crystalline peak (I_{002}–I_{AM}) and total intensity of the peak (I_{002}), i.e., the fact that the peak width of the amorphous region is larger than in the crystalline phase is ignored. However, the trends in the apparent CI values obtained by both techniques are very similar (Fig. 2 and Table 2). For the mildly pretreated samples the apparent CIs are approximately linearly proportional to the cellulose concentration in the samples. When the harsher pretreatments are applied and the resulting cellulose fraction becomes higher than 55%, CIs stabilize and stop growing with the increase in the cellulose content in the samples. This probably reflects the fact that the more vigorous pretreatments lead to unstructuring of the cellulose bundles and to an effective decrease cellulose crystallinity of the biomass. However, since the cellulose fraction within the samples becomes larger, the total CIs stagnate at approximately the same levels.

Next, in order to better understand the morphological changes caused by the pretreatments, secondary electron images (SEI) of bagasse samples were obtained using Field Emission Scanning Electron Microscopy (FESEM) before and after the various pretreatment steps. Sugarcane bagasse is composed of fibers and pith cells (Fig. 3). The fibers are indicated by the yellow arrows in Fig. 3A. Thus, most of the solid material that resists the treatment consists of fibers and, for that reason the comparison of the untreated bagasse and pretreated samples will always refer to the fibrous regions. In untreated samples, the fiber bundles are covered by a dense surface layer (Supplementary material, Fig. S1 A and B). This surface layer is being gradually removed by the pretreatments, as shown in Fig. 3B (Hyd_60′ + Org_150′). This effect was observed for the samples that underwent organosolv pretreatment (Supplementary material, Fig. S1C). Another effect of the pretreatment is the separation of fiber bundles in the bagasse structure presumably caused by the sample delignification. Lignin acts as an adhesive that joins the fibers together and, when it is removed, the fibers lose their tightly packed assembly and start to separate. Thus, unstructuring of the bundles can be clearly observed (Fig. 3B). This effect was also observed in bagasse samples subjected to other pretreatment methods (Mosier et al., 2005; Rezende et al., 2011) and is more pronounced in more delignified samples.

Moreover, the treatments studied here lead to the formation of deposits of particulate material on the surface, which can form smaller or larger droplets. In particular, the droplets indicated by the blue arrows in Fig. 3B (Hyd_60′ + Org_150′) are similar to the lignin deposits observed in different lignocellulosic samples that underwent steam explosion, diluted acid or organosolv pretreatments (Heiss-Blanquet et al., 2011; Koo et al., 2012; Selig et al., 2007). Formation of the deposits is assigned to the removal of lignin from within the cell walls, followed by its redeposition at the surface of the biomass. Considering the pretreatment conditions applied in the current work, the lignin deposits are more frequently observed in the samples after organosolv pretreatment: Org_50′, Org_100′, Org_150′, Hyd_30′ + Org_50′, Hyd_30′ + Org_100′, Hyd_30′ + Org_150′, Hyd_60′ + Org_50′, Hyd_60′ + Org_100′ and Hyd_60′ + Org_150′ (Supplementary material, Fig. S1D and E). Notably, lignin droplets deposits are not observed in

Table 3
Cellulose conversion after 72 h of enzymatic hydrolysis for untreated sugarcane bagasse and bagasse samples, which underwent hydrothermal, organosolv and hydrothermal/organosolv treatments after 72 h of enzymatic hydrolysis. Standard deviations were computed from the average values of duplicate determinations.

	Cellulose conversion	
Pretreatments	Enzymatic hydrolysis yields, %[*,#]	Total saccharification yields, %[*,$]
Untreated	22.0 ± 0.2	22.0 ± 0.2
Hyd_1′	32.8 ± 0.4	29.8 ± 0.4
Hyd_30′	37.9 ± 4.0	29.6 ± 3.1
Hyd_45′	43.0 ± 5.0	31.3 ± 3.3
Hyd_60′	37.5 ± 0.6	26.5 ± 0.4
Org_50′	51.0 ± 16.0	35.5 ± 11.1
Org_100′	63.0 ± 6.0	35.0 ± 3.6
Org _150′	69.0 ± 5.0	36.8 ± 2.5
Hyd_30′+ Org_50′	48.0 ± 7.0	29.9 ± 4.3
Hyd_30′+ Org_100′	76.8 ± 12.0	42.9 ± 6.9
Hyd_30′+ Org _150′	72.0 ± 5.0	36.8 ± 2.4
Hyd_60′+ Org_50′	47.0 ± 4.0	26.7 ± 2.3
Hyd_60′+ Org_100′	74.0 ± 7.0	39.8 ± 3.7
Hyd_60′+ Org _150′	75.0 ± 8.0	37.0 ± 3.9

[*] Yield values are expressed as an average ± standard deviation of experimental duplicates.

[#] The enzymatic hydrolysis yield was calculated as a percentage of cellulose conversion into glucose caused by the enzymatic hydrolysis based on the amount of cellulose in the pretreated biomass.

[$] The total saccharitication yield was computed as a fraction of cellulose in the original untreated biomass, which was converted into glucose by the action of the enzymes after accounting for loses of glucans caused by the applied pretreatments.

the samples that underwent hydrothermal pretreatment only.

Hydrothermally pretreated samples for a short period of time (Hid_1′) have morphologies that are very similar to the untreated bagasse (Fig. 3C and Supplementary material, Fig. S2A. At higher magnifications, however, small droplets distributed on the surface can be observed, indicating lignin redeposition even under mild conditions. These droplets are not observed in the untreated bagasse samples. The gross similarities between these pretreated samples and the untreated samples are in agreement with the composition data presented in Table 1 and also with the very similar hydrolysis yields obtained from these samples (Table 3). It is important to notice the morphological differences between the hydrothermally pretreated samples (Hyd_1′, Fig. 3C) and the samples that underwent combined pretreatments (Hyd_60′ + Org_150′, Fig. 3B), which highlight the contribution of the organosolv treatment to the unstructuring of the sugarcane bagasse samples.

The samples that underwent only hydrothermal pretreatment: Hyd_30′, Hyd_45′and Hyd_60′, all have very similar morphologies, with the fiber surface layers being removed and the cellulose bundles beginning to separate (Fig. 3D). Deposition of particulate material at the surface of these samples is very modest, which indicates that this effect is indeed characteristic of more severe pretreatments. Fig. 3E (Hyd_60′) shows the transversal section of a fiber bundle in this sample, with the green arrow indicating a fiber detaching from the bundle surface. Although showing some evidence of unstructuring, most of the fibers are still strongly bound together. The outermost fibers are the first to detach from the bundle, which becomes thinner as the pretreatment progresses.

Samples that underwent combined pretreatments, Hyd_60′ + Org_50′ (Supplementary material, Fig. S2 B and C) and Hyd_60′ + Org_150′ (Fig. 3F and Supplementary material, Fig. S2 D) are considerably more unstructured. The amount of particulate material deposited on the surface is much higher, both in the form of droplets or of cell wall pieces removed from some areas. In the case of the sample Hyd_60′ + Org_150′, the dismantling of the fiber bundles is slightly more advanced as compared to the other samples (Fig. 3F). Furthermore, due to the significant removal of the outermost layers of the fiber bundle, thinner cellulose fibrils are becoming more exposed (Fig. 3F). One of these cellulose fibrils is indicated by the red arrow in Fig. 3F and many others are evident at the surface of the main fiber. In some areas of the samples pretreated under the most severe conditions, even thinner fibrils can be observed in highly amplified images. This becomes possible because the contour of the cellulose fibrils is much better defined, mainly due to the removal of the layers that cover the fibrils, but also of the interstitial material between neighboring fibers.

Regarding the effects of the organosolv pretreatments time, the differences comparing samples Org_50′ or Org_150′ conditions were not detected using the FESEM technique. The images obtained from these samples at different amplifications show a very similar morphology in both cases with comparable amounts of residues deposited on the surface and a similar separation of neighboring fiber bundles (Supplementary material, Fig. S2).

A large number of images obtained by FESEM provided a body of evidence for the reallocation of lignin caused by the pretreatments in the bagasse samples. To confirm this and to obtain more detailed information about the lignin-rich areas in the cell wall, confocal laser scanning microscopy technique (CLSM) was applied. CLSM is a fluorescence imaging technique that allows the chemical mapping of chromophores on the various sample layers, both on the surface and in the inner regions, by adjusting the focal plane. It allows measuring the emission spectra and also the fluorescence decay time in each point of the image. Since the emitting fluorophore has a characteristic fluorescence decay time that depends on its microenvironment, evidence of chemical changes, such as the molecular arrangement of fluorophores, can be obtained (Gerritsen et al., 2002). In the case of plant biomass samples, the lignin can be used as a chromophore. Previous studies showed that both lignin degradation (Singh et al., 2006; Speranza et al., 2009) and redistribution (Chundawat et al., 2011) in the cell wall can be caused by pretreatments. Lignin represents around 25% of the dry sugarcane bagasse composition and any change in its molecular arrangement, for instance agglomeration or redeposition, can be easily detected by CLSM. Our recent study showed that the emission spectrum and the time decay of lignin are strongly modified by acid-alkali pretreatments (Coletta et al., 2013). In addition, the excitation using the two-photon technique was demonstrated to be essential to obtain information on lignin agglomeration. In our experiments the confocal plane was adjusted to obtain information from the surface of the bagasse fibers, thus allowing consistent comparison among all the analyzed samples (Supplementary material, Fig. S3). Each pixel shown in these images contains information about the emission spectrum of lignin at that particular position. Untreated sugarcane bagasse basically emits in a blue spectrum (400–500 nm range; Fig. 4A) and very few spectrum alterations are observed in replicates. The samples hydrothermically pretreated for 1 min do not present significant spectral changes (Supplementary material, Fig. S4A), when compared to the untreated samples. However, the samples pretreated for 30 min, 45 min (Supplementary material, Fig. S4 B) and 60 min show gradual alterations, which are becoming more evident as the reaction time increases. In general, all samples begin emitting at the longer wavelength region between green and red (500–700 nm). Longer wavelength and thus lower energy emissions are associated with the formation of complex molecular aggregates. These spectral changes report a deconstruction in the well-structured lignin assembly within the plant cell wall, similar to the ones observed in studies involving sugarcane bagasse treated with diluted acid (McDonough, 1993). This similarity can be explained by the acid catalysis involved in the hydrothermal process at high temperatures, caused by the release of acetic acid as a by-product of hemicelluloses hydrolysis.

Although the total lignin content in the biomass samples after the hydrothermal pretreatments stays virtually constant (Table 1), the CLSM images reveal that the hydrothermal treatment causes considerable redistribution of lignin (Fig. 4), which also can be associated with changes between soluble and insoluble lignin fractions.

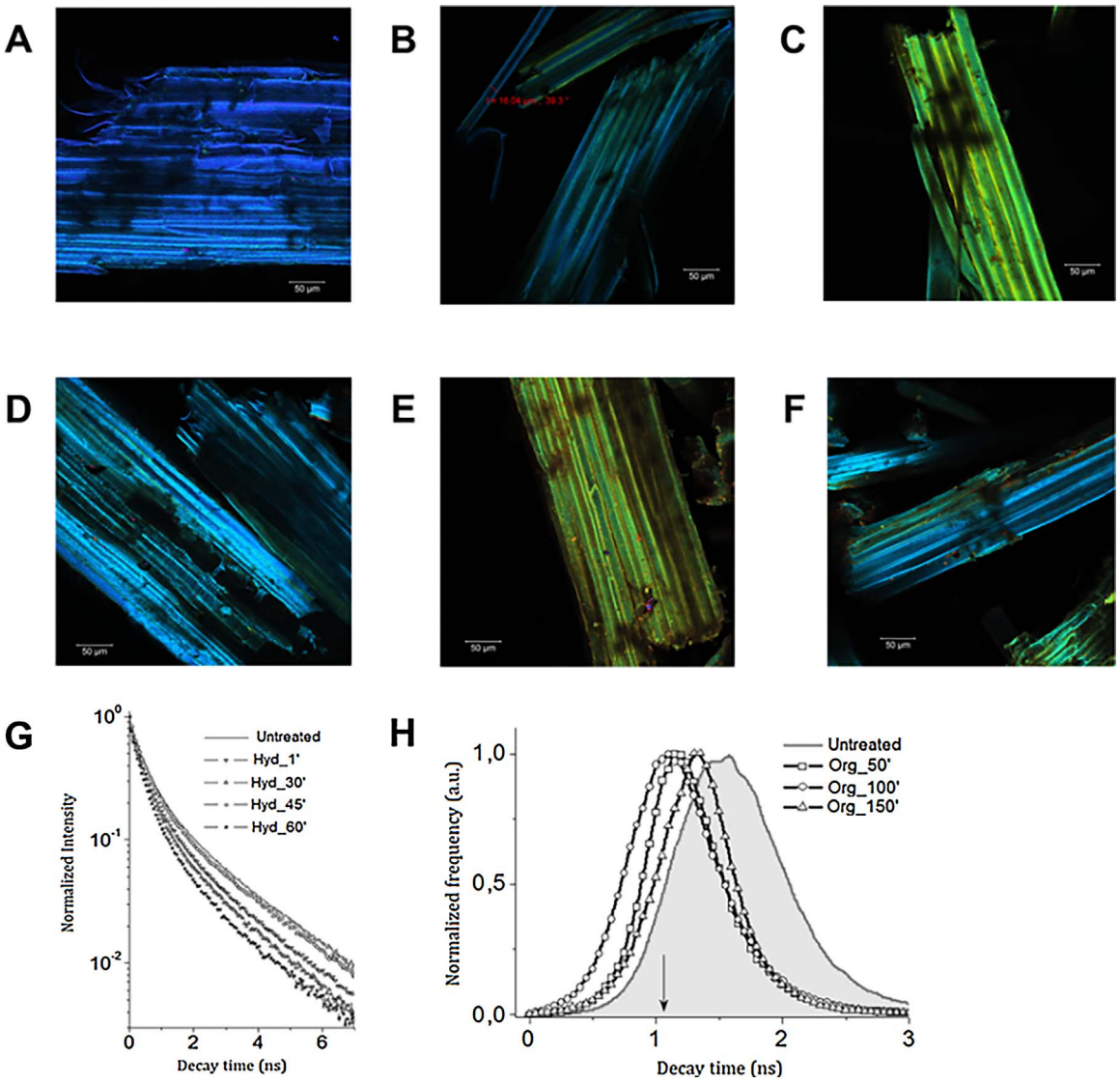

Fig. 4. CLSM image of sugarcane bagasse samples in a spectral mode. (A) untreated sugarcane bagasse, (B) Hyd_30′, (C) Hyd_60′, (D) Org_50′, (E) Org_100′ and (F) Org_150′. Comparison of the fluorescence decay curves for the untreated sample and sample after hydrothermal pretreatment given in a semi-log scale (G). The decay curves can be deconvoluted in two processes, one with a short decay time (t1; below 2 ns) and a long decay time (t2; longer than 2 ns) for all samples. (H) Normalized distributions of average lifetime calculated for each pixel of the image FLIM for the samples after organosolv pretreatment. The curve from the reference untreated sample (filled in gray) is displaced toward longer decay times. The arrow corresponds to the average position of distribution for the hydrothermally pretreated sample after 60 min.

Consistent with our FESEM results, the CLSM analysis confirms that the samples that underwent hydrothermal treatments do not present lignin droplets accumulated at their surfaces. Furthermore, in line with the ssNMR analysis (Fig. 1A), hydrothermal pretreatments under these conditions are not associated with significant structural chemical alterations of lignin. However, the spectral images obtained in samples with longer hydrothermal treatment times have sharper two photons fluorescence spectrum, characteristic of molecular aggregation within the cell walls, this indicates changes in the lignin structure of the pretreated plant cell walls (Fig. 4B and C).

Coletta et al. observed a similar behavior in bagasse samples acid pretreated with a 1% H_2SO_4 solution (Coletta et al., 2013). The pretreatment did not remove lignin, but induced molecular rearrangements, generating lignin aggregates (Coletta et al., 2013). The fact that the average lifetime distributions shifts towards shorter lifetimes, without altering the format of the distribution area (Fig. 4G), is associated to an increase in the molecular aggregation (Coletta et al., 2013), and higher aggregation of the emitting molecules results in a decreased decaying fluorescence time. The shorter fluorescence lifetimes can be explained by the migration of the excited state through Foerster-type energy transfer processes within the aggregates (Foerster, 1959). The stronger the aggregation process is the higher is the probability of finding a non-emitting light center, which leads to the reduced lifetime. This explains shortening of the lignin fluorescence lifetime under two photons excitation.

As for organosolv pretreatments (Fig. 4D–F), 3 out of 5 measurements of the samples after a 50 min reaction time show predominantly emission in the blue region, whereas the remaining 2 revealed fluorescence emission predominantly in the green region of the visible light spectrum (Fig. 4 D). Thus, deconstruction and/or removal of lignin for this particular pretreatment seem to be inhomogeneous. However, the samples pretreated under organosolv conditions for 100 min showed predominant emission in the green region (Fig. 4E). Furthermore, the samples treated for 150 min showed mostly emission in the blue spectral region (Fig. 4F), which may indicate the dissolution of lignin agglomerations and their extraction by the organic solvent. In contrast, samples hydrothermally treated for 60 min (Fig. 4C) presented only rearrangements of lignin (emission in green spectral region), but their dissolution has not been observed. Therefore, the return to the blue light emission after the organosolv pretreatment for 150 min could be

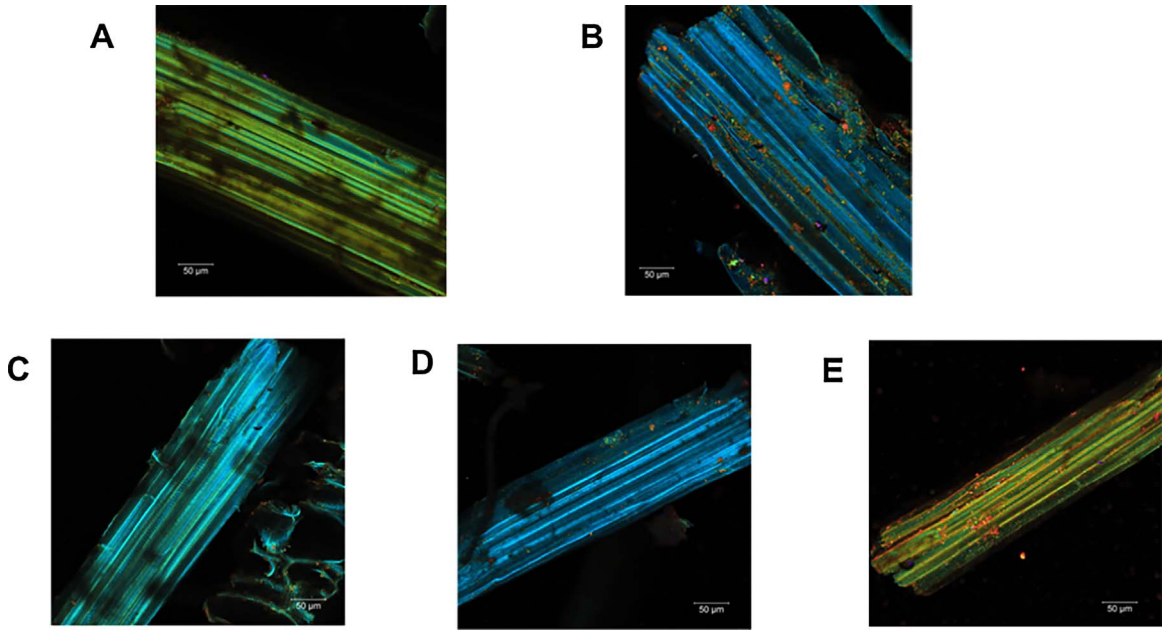

Fig. 5. CLSM image of sugarcane bagasse samples in a spectral mode. Combined pretreatments. (A) Hyd_30′ + Org_50′ (B) Hyd_30′ + Org_150′ (C) Hyd_60′ + Org_50′ (D) Hyd_60′ + Org_100′ (E) Hyd_60′ + Org_150′.

an evidence of the simultaneous extraction and dissolution of lignin from the bagasse samples (Table 1).

Considering the alterations in decay times for the organosolv pretreated samples (Fig. 4H), one can observe that the decay times for all the samples are shorter when compared to the untreated samples. However, the lifetime shift toward shorter times is partially reversed for the sample treated with organosolv for 150 min, indicating that the lignin aggregates in this particular sample were reduced in number, when compared to other organosolv pretreated samples and also to a sample that was hydrothermally pretreated for 60 min (indicated by arrow in Fig. 4H). According to Coletta et al. (2013), a shift toward longer decay times is expected, when lignin concentration in the cell walls is reduced. It is possible to note the dissolution of the agglomerates and the removal of lignin based on the lifetime distribution, based on their proximity to the reference sample. The compositional analysis of the pretreated bagasse samples showed an important lignin removal in samples hydrothermally treated for 30 min, combined with a subsequent organosolv step for 150 min. The final lignin amount in this sample was only 10.9% against 29.0% in the untreated bagasse sample. The effects of the combined treatment with a hydrothermal step for 30 min, followed by the organosolv step, are given in Fig. 5. The sample pretreated by the hydrothermal process for 30 min followed by organosolv pretreatment for 50 min (Hyd_30′ + Org_50′ shown in Fig. 5A) has a surface covered by lignin deposition, resulting in a continuous green emitting throughout the surface. Interestingly, for the samples treated in this hydrothermal process followed by organosolv for 100 and 150 min (Hyd_30′ + Org_100′and Hyd_30′ + Org_150′), the accumulated lignin was partly removed and the remaining lignin domains took the form of large isolated clusters distributed on the surface, as can be observed by the red points, in the form of spherical aggregates, as can be observed in these images (Hyd_30′ + Org_100′, Fig. 5B and Hyd_30′ + Org_100′, Supplementary Material, Fig. S4 B).

There is a higher tendency for lignin removal from bagasse surface for the samples pretreated under Hyd_60′ + Org_50′ and Hyd_60′ + Org_100′conditions (Fig. 5C and D, respectively), as indicated by the observed strong emission contribution in the blue spectral region. The sample Hyd_60′ + Org_150′ (Fig. 5E) lead to lignin distributed on the surface with strong tendency to form more lignin agglomerates. These results suggest that the deconstruction of lignin leading to the formation aggregates within the cell wall by long hydrothermal pretreatments may turn it difficult their subsequent dissolution by the organic solvent. Therefore, there could be an optimal ratio between the duration of hydrothermal treatment and the solvent effects leading to dissolution and removal of lignin aggregates. This hypothesis will be addressed in future studies. Both the SEM and the CLSM images of the samples (Figs. 3–5), jointly confirm the reallocation of lignin caused by the pretreatments in the bagasse structure and provide an explanation for changes in lignin composition.

3.3. Enzymatic hydrolysis

Frequently, the efficiency of a pretreatment is not being restricted exclusively to chemical composition and physical characteristics of the pretreated biomass and is reported in terms of its influence on enzymatic hydrolysis released glucose yield. Here, the yield of enzymatic hydrolysis was first calculated based on the cellulose fraction of each pretreated sample used in the experiment (called herein an enzymatic hydrolysis yield) (Table 3). Next, the calculations for the total conversion of cellulose with respect to the cellulose fraction in the original non-pretreated samples were performed, taking into consideration the losses caused by each treatment (termed a total saccharification yield) (Table 3). Since a partion of glucan fraction tends to be lost during pretreatment steps, the total saccharification yields are generally lower than the enzymatic hydrolysis yields.

As one can observe in Table 3, direct enzymatic conversion of the untreated sugarcane bagasse to glucose is quite low. An access of the enzymes to the substrate, cellulose, embedded in the complex hemicelluloses and lignin matrix is restricted and this turns unpretreated biomass into a highly recalcitrant substrate. The sugarcane bagasse that underwent a pretreatment process tends to present a higher conversion rate of polysaccharides to fermentable sugars. Under conditions employed in the present study, this could be verified mainly for the pretreatments involving organosolv ethanol/water and for the reactions with the duration of more than 100 min at 190 °C which results in a significantly enhanced yield of enzymatic hydrolysis raising from 22.0% for the untreated sugarcane bagasse to 76.8% in the combined Hyd_30′ + Org_100′ treatment. The results for the combined Hyd_30′ + Org_150′ and Hyd_60′ + Org_150′ pretreatments were also impressive, providing a conversion yields of 72.0% and 75.0%, respectively.

It is important to notice the differences in the efficiencies of enzymatic hydrolysis between the samples pretreated under the Hyd_60′, Org_150′ and Hyd_60′ + Org_150′ pretreatment conditions, highlighting the contribution of each pretreatment for the final state of unstructuring and degradation of the plant cell walls. Under conditions of Hyd_60′ pretreatment, the characteristic molecular aggregation of lignin within the cell walls has been observed, indicating changes in the lignin structure (Fig. 3Figs. 3E and Fig. 44C), which might contribute to the better access of hydrolytic enzymes to the pretreated bagasse. But for this particular pretreatment, the lignin, although modified and redeposited, continues to be present in the biomass (Fig. 1A). For Org_150 pretreatment the dissolution and extraction of lignin take place (Fig. 1B and Table 1), making the enzymatic hydrolysis step easier and more efficient. The combination of these two pretreatment leads to the significant lignin removal and chemical modification leading to the formation of aggregates during the hydrothermal step and their partial dissolution by the organic solvent at the second, organosolv pretreatment step, thus further improving the efficiency of enzymatic hydrolysis after pretreatment (Table 3). Organosolv pretreatments prove themselves very effective in improving the enzymes accessibility during the hydrolysis phase, presumably due to the lignin removal, as indicated by their chemical composition analysis and ^{13}C solid-state NMR results. Finally, the combined hydrothermal pretreatments (for 30 and 60 min) followed by organosolv for 100–150 min studied in this work imprint very similar substrate morphologies, which is consistent with the fact that these samples demonstrate comparable enzymatic hydrolysis yields on the order of 75% (Table 3).

4. Conclusions

By using the arsenal of the physical techniques and chemical composition analyses, it was possible to reveal structural modifications and chemical composition changes caused by the hydrothermal and organosolv pretreatments in the sugarcane bagasse samples. Combined biomass physical structure studies using FESEM, CLSM, FLIM, ssNMR and LC-based chemical composition analyses conducted in this work confirm that under the applied conditions, the organosolv pretreatment efficiently removed lignin from the sugarcane bagasse leading to increased concentration of cellulose in the pretreated substrate, as opposed to hydrothermal pretreatment which mainly caused a disorder in the lignin arrangement. Moreover, as verified by FESEM, CLSM and FLIM, the organosolv pretreatment alone and its combination with the hydrothermal pretreatment (with the residence time of 30 and 60 min) resulted in lignin degradation, rearrangement and non-homogeneous deposition of significant quantities of lignin on the surface of the substarate. Such two-step pretreatment removed up to 75% of hemicelluloses and up to 62% of lignin from the sugarcane bagasse samples. The cellulose conversion yield was 72% for the samples after combined, Hyd_30′ + Org_150′ pretreatment, representing a considerable increase in comparison to 22% yield for untreated bagasse. These pretreatments were shown to result in the loss of cohesion between adjacent cell wall layers, exposure of the cellulose fibers and dismanteling of cellulose bundles, thus facilitating enzymatic hydrolysis. Both X-ray diffraction and ssNMR reveal that cellulose crystallinity stagnates when the cellulose concentration increases above 60% as a result of lignin removal and hemicellulose solutibization, which coinsides with the conditions of increased enzymatic hydrolysis yields. A combination of physical techniques and chemical analytical methods allowed us to obtain comprehensive information, regarding lignin disposition in the biomass and cellulose fibril structures, thus making possible a better understanding of the morphological changes of the biomass samples caused by the pretreatments and shed light on their influence on enzymatic hydrolysis.

Competing interests

The authors declare that they have no competing interests.

Acknowledgements

The authors would like to thank LME/LNNano/CNPEM for the technical support during the electron microscopy work, EMBRAPA Instrumentação for the technical support during nuclear resonance magnetic work and CAPES. This research was supported by the Fundação de Amparo à Pesquisa do Estado de São Paulo (FAPESP) via grants 10/52362-5 and 15/13684-0 and the Conselho Nacional de Desenvolvimento Científico e Tecnológico (CNPq) via grants 140667/2015-6, 158752/2015-5, 405191/2015-4, 303988/2016-9, 440977/2016-9 and 423693/2016-6.

Appendix A. Supplementary data

Supplementary data associated with this article can be found, in the online version, at https://doi.org/10.1016/j.indcrop.2018.01.014.

References

Achyuthan, K.E., Achyuthan, A.M., Adams, P.D., Dirk, S.M., Harper, J.C., Simmons, B.A., Singh, A.K., 2010. Supramolecular self-assembled chaos: polyphenolic lignin's barrier to cost-effective lignocellulosic biofuels. Molecules 15 (12), 8641–8688. http://dx.doi.org/10.3390/molecules15118641.

Bernardinelli, O.D., Lima, M.A., Rezende, C.A., Polikarpov, I., Ribeiro deAzevedo, E., 2015. Quantitative 13C multiCP solid-state NMR as a tool for evaluation of cellulose crystallinity index measured directly inside sugarcane biomass. Biotechnol. Biofuels 8 (1), 110. http://dx.doi.org/10.1186/s13068-015-0292-1.

Brodeur, G., Yau, E., Badal, K., Collier, J., Ramachandran, K.B., Ramakrishnan, S., 2011. Chemical and physicochemical pretreatment of lignocellulosic biomass: a review. Enzyme Res. 2011http://dx.doi.org/10.4061/2011/787532. Article ID 787532, 17 pages.

Chundawat, S.P.S., Donohoe, B.S., Sousa, L.C., Elder, T., Agarwal, U.P., Lu, F., Ralph, J., Himmel, M.E., Balan, V., Dale, B.E., 2011. Multi-scale visualization and characterization of lignocellulosic plant cell wall deconstruction during thermochemical pretreatment. Energy Environ. Sci. 4 (3), 973–984. http://dx.doi.org/10.1039/C0EE00574F.

Coletta, V.C., Rezende, C.A., da Conceição, F.R., Polikarpov, I., Guimarães, F.E.G., 2013. Mapping the lignin distribution in pretreated sugarcane bagasse by confocal and fluorescence lifetime imaging microscopy. Biotechnol. Biofuels 6 (1), 43. http://dx.doi.org/10.1186/1754-6834-6-43.

Dias, M.O.S., Junqueira, T.L., Cavalett, O., Cunha, M.P., Jesus, C.D.F., Rossell, C.E.V., Filho, R.M., Bonomi, A., 2012. Integrated versus stand-alone second generation ethanol production from sugarcane bagasse and trash. Bioresour. Technol. 103 (1), 152–161. http://dx.doi.org/10.1016/j.biortech.2011.09.120.

Foerster, T.H., 1959. 10th spiers memorial lecture. transfer mechanisms of electronic excitation. Discuss. Faraday Soc. 27, 7–17. http://dx.doi.org/10.2307/3583604.

Gerritsen, H.C., Asselbergs, M.A.H., Agronskaia, A.V., Van Sark, W.G.J.H.M., 2002. Fluorescence lifetime imaging in scanning microscopes: acquisition speed, photon economy and lifetime resolution. J. Microsc. 206 (3), 218–224. http://dx.doi.org/10.1046/j.1365-2818.2002.01031.x.

Gilarranz, M.A., Rodriguez, F., Oliet, M., 2000. Lignin behavior during the autocatalyzed methanol pulping of Eucalyptus globulus – changes in molecular weight and functionality. Holzforschung 54 (4), 373–380. http://dx.doi.org/10.1515/HF.2000.064.

Hallac, B.B., Sannigrahi, P., Pu, Y., Ray, M., Murphy, R.J., Ragauskas, A.J., 2009. Biomass characterization of Buddleja davidii: a potential feedstock for biofuel production. J. Agric. Food Chem. 57 (4), 1275–1281. http://dx.doi.org/10.1021/jf8030277.

Heiss-Blanquet, S., Zheng, D., Ferreira, N.L., Lapierre, C., Baumberger, S., 2011. Effect of pretreatment and enzymatic hydrolysis of wheat straw on cell wall composition, hydrophobicity and cellulase adsorption. Bioresour. Technol. 102 (10), 5938–5946. http://dx.doi.org/10.1016/j.biortech.2011.03.011.

Himmel, H.E., Ding, S.Y., Johnson, D.K., Adney, W.S., Nimlos, M.R., Brady, J.W., Foust, T.D., 2007. Biomass recalcitrance: engineering plants and enzymes for biofuels production. Science 315 (5813), 804–807. http://dx.doi.org/10.1126/science.1137016.

Hu, Z., Foston, M.B., Ragauskas, A., 2011. Biomass characterization of morphological portions of alamo switchgrass. J. Agric. Food Chem. 59 (14), 7765–7772. http://dx.doi.org/10.1021/jf104844r.

Kartal, S.N., Hwang, W.J., Imamura, Y., 2007. Water absorption of boron-treated and heat-modified wood. J. Wood Sci. 53 (5), 454–457. http://dx.doi.org/10.1007/s10086-007-0877-9.

Koo, B.W., Min, B.C., Gwak, K.S., Lee, S.M., Choi, J.W., Yeo, H., Choi, I.G., 2012. Structural changes in lignin during organosolv pretreatment of Liriodendron tulipifera and the effect on enzymatic hydrolysis. Biomass Bioenergy 42, 24–32. http://dx.

doi.org/10.1016/j.biombioe.2012.03.012.
Kumar, P., Barrett, D.M., Delwiche, M.J., Stroeve, P., 2009. Methods for pretreatment of lignocellulosic biomass for efficient hydrolysis and biofuel production. Ind. Eng. Chem. Res. 48 (8), 3713–3729. http://dx.doi.org/10.1021/ie801542g.
Lima, M.A., Gomez, L.D., Steele-King, C.G., Simister, R., Bernardinelli, O.D., Carvalho, M.A., Polikarpov, I., 2014. Evaluating the composition and processing potential of novel sources of Brazilian biomass for sustainable biorenewables production. Biotechnol. Biofuels 7 (1), 10. http://dx.doi.org/10.1186/1754-6834-7-10.
Ma, X.J., Yang, X.F., Zheng, X., Lin, L., Chen, L.H., Huang, L.L., Cao, S.L., 2014. Degradation and dissolution of hemicelluloses during bamboo hydrothermal pretreatment. Bioresour. Technol. 161, 215–220. http://dx.doi.org/10.1016/j.biortech.2014.03.044.
Maeda, R.N., Serpa, V.I., Rocha, V.A.L., Mesquita, R.A.A., Santa Anna, L.M.M., De Castro, A.M., Polikarpov, I., 2011. Enzymatic hydrolysis of pretreated sugar cane bagasse using Penicillium funiculosum and Trichoderma harzianum cellulases. Process Biochem. 46 (5), 1196–1201. http://dx.doi.org/10.1016/j.procbio.2011.01.022.
McDonough, T.J., 1993. The chemistry of organosolv delignification. TAPPI J. 76 (8), 186–193.
Mosier, N., Wymanb, C., Dalec, B., Elanderd, R., Lee, Y., Holtzapplef, M., Ladisch, M., 2005. Features of promising technologies for pretreatment of lignocellulosic biomass. Bioresour. Technol. 96 (6), 673–686. http://dx.doi.org/10.1016/j.biortech.2004.06.025.
Nakagame, S., Chandra, R.P., Sadller, J.N., 2011. The influence of lignin on the enzymatic hydrolysis of pretreated biomass substrate. In: In: Zhu, J.Y., Zhang, X., Pan, X.J. (Eds.), Sustainable Production of Fuels, Chemicals, and Fibers from Forest Biomass 1067. American Chemical Society, New York, pp. 145–167. http://dx.doi.org/10.14288/1.0071453. cap. 6.
Novo, L.P., Gurgel, L.V., Marabezi, K., Curvelo, A.A., 2011. Delignification of sugarcane bagasse using glycerol–water mixtures to produce pulps for saccharification. Bioresour. Technol. 102 (21), 10040–10046. http://dx.doi.org/10.1016/j.biortech.2011.08.050.
Park, Y., Doherty, W.O., Halley, P.J., 2008. Developing lignin-based resin coatings and composites. Indus. Crops Prod. 27 (2), 163–167. http://dx.doi.org/10.1016/j.indcrop.2007.07.021.
Park, S., Baker, J.O., Himmel, M.E., Parilla, P.A., Johnson, D.K., 2010. Cellulose crystallinity index: measurement techniques and their impact on interpreting cellulase performance. Biotechnol. Biofuels 3 (1), 10. http://dx.doi.org/10.1186/1754-6834-3-10.
Paul, Eldor A., 2014. Soil Microbiology, Ecology and Biochemistry. Academic press.
Pu, Y., Ziemer, C., Ragauskas, A.J., 2006. CP/MAS 13C NMR analysis of cellulase treated bleached softwood kraft pulp. Carbohydr. Res. 341 (5), 591–597. http://dx.doi.org/10.1016/j.carres.2005.12.012.
Rezende, C.A., de Lima, M.A., Maziero, P., deAzevedo, E.R., Garcia, W., Polikarpov, I., 2011. Chemical and morphological characterization of sugarcane bagasse submitted to a delignification process for enhanced enzymatic digestibility. Biotechnol. Biofuels 4 (1), 54. http://dx.doi.org/10.1186/1754-6834-4-54.
Rocha, G.J.M., Martin, C., Soares, I.B., Maior, A.M.S., Baudel, H.M., de Abreu, C.A.M., 2011. Dilute mixed-acid pretreatment of sugarcane bagasse for ethanol production. Biomass Bioenerg. 35, 663–670. http://dx.doi.org/10.1016/j.biombioe.2010.10.018.
Roos, A.A., Persson, T., Krawczyk, H., Zacchi, G., Stålbrand, H., 2009. Extraction of water-soluble hemicelluloses from barley husks. Bioresour. Technol. 100 (2), 763–769. http://dx.doi.org/10.1016/j.biortech.2008.07.022.
Sannigrahi, P., Miller, S.J., Ragauskas, A.J., 2010. Effects of organosolv pretreatment and enzymatic hydrolysis on cellulose structure and crystallinity in Loblolly pine. Carbohydr. Res. 345 (7), 965–970. http://dx.doi.org/10.1016/j.carres.2010.02.010.
Sarkanen, S., Teller, D.C., Hall, J., McCarthy, J.L., 1981. Lignin 18. Associative effects among organosolv lignin components. Macromolecules 14, 426–434. http://dx.doi.org/10.1021/ma50003a037.
Selig, M.J., Viamajala, S., Decker, S.R., Tucker, M.P., Himmel, M.E., Vinzant, T.B., 2007. Deposition of lignin droplets produced during dilute acid pretreatment of maize stems retards enzymatic hydrolysis of cellulose. Biotechnol. Progr. 23 (6), 1333–1339. http://dx.doi.org/10.1021/bp0702018.
Sheehan, J., Himmel, M., 1999. Enzymes, energy, and the environment: a strategic perspective on the U.S. Department of Energy's research and development activities for bioethanol. Biotechnol. Progr. 15, 817–827. http://dx.doi.org/10.1021/bp990110d.
Singh, A.P., Schmitt, U., Möller, R., Dawson, B.S., Koch, G., 2006. Ray tracheids in Pinus radiata are more highly resistant to soft rot as compared to axial tracheids: relationship to lignin concentration. Wood Sci. Technol. 40 (1), 16. http://dx.doi.org/10.1007/s00226-005-0056-3.
Soccol, C.R., Vandenberghe, L.P.S., Medeiros, A.B.P., Karp, S.G., Buckeridge, M., Ramos, L.P., Pitare-lo, A.P., Ferreira-Leitão, V., Gottschalk, L.M.F., Ferrara, M.A., Bom, E.P.S., Moraes, P., Araújo, J.A., Torres, F.A.G., 2010. Bioethanol from lignocelluloses: status and perspectives in Brazil. Bioresour. Technol. 101 (13), 4820–4835. http://dx.doi.org/10.1016/j.biortech.2009.11.067.
Speranza, M., Guitérrez, A., Del Río, J.C., Bettucci, L., Martínez, A.T., Martínez, M.J., 2009. Sterols and lignin in Eucalyptus globulus Labill. wood: spatial distribution and fungal removal as revealed by microscopy and chemical analyses. Holzforschung 63 (3), 362–370. http://dx.doi.org/10.1515/HF.2009.041.
Taherzadeh, M., Karimi, K., 2007. Acid-based hydrolysis processes for ethanol from lignocellulosic materials: a review. BioResources 2 (3), 472–499.
Templeton, D.W., Scarlata, C.J., Sluiter, J.B., Wolfrum, E.J., 2010. Compositional analysis of lignocellulosic feedstocks. 2. Method uncertainties. J. Agric. Food Chem. 58 (16), 9054–9062. http://dx.doi.org/10.1021/jf100807b.
Tunc, M.S., Van Heiningen, A.R., 2011. Characterization and molecular weight distribution of carbohydrates isolated from the autohydrolysis extract of mixed southern hardwoods. Carbohydr. Polym. 83 (1), 8–13. http://dx.doi.org/10.1016/j.carbpol.2010.07.015.
Vázquez, M.J., Garrote, G., Alonso, J.L., Domínguez, H., Parajó, J.C., 2005. Refining of autohydrolysis liquors for manufacturing xylooligosaccharides: evaluation of operational strategies. Bioresour. Technol. 96 (8), 889–896. http://dx.doi.org/10.1016/j.biortech.2004.08.013.
Vallejos, M.E., Zambon, M.D., Area, M.C., Curvelo, A.A.S., 2012. Low liquid-solid ratio (LSR) hot water pretreatment of sugarcane bagasse. Green Chem. 14 (7), 1982–1989. http://dx.doi.org/10.1039/c2gc35397k.
Wickholm, K., Larsson, P.T., Iversen, T., 1998. Assignment of non-crystalline forms in cellulose I by CP/MAS 13C NMR spectroscopy. Carbohydr. Res. 312 (3), 123–129. http://dx.doi.org/10.1016/S0008-6215(98)00236-5.
Wingren, A., Galbe, M., Roslander, C., Rudolf, A., Zacchi, G., 2005. Effect of reduction in yeast and enzyme concentrations in a simultaneous – saccharification-andfermentation-based bioethanol process: technical and economic evaluation. Appl. Biochem. Biotechnol. 122 (1–3), 485–499. http://dx.doi.org/10.1385/ABAB:122:1-3.
Xing, R., Qi, W., Huber, G.W., 2011. Production of furfural and carboxylic acids from waste aqueous hemicellulose solutions from the pulp and paper and cellulosic ethanol industries. Energy Environ. Sci. 4 (6), 2193—2205. http://dx.doi.org/10.1039/C1EE01022K.
Yu, G., Yano, S., Inoue, H., Inoue, S., Endo, T., Sawayama, S., 2010. Pretreatment of rice straw by a hot-compressed water process for enzymatic hydrolysis. Appl. Biochem. Biotechnol. 160 (2), 539–551. http://dx.doi.org/10.1007/s12010-008-8420-z.
Yu, Q., Zhuang, X., Lv, S., He, M., Zhang, Y., Yuan, Z., Qi, W., Wang, Q., Wang, W., Tan, X., 2013. Liquid hot water pretreatment of sugarcane bagasse and its comparison with chemical pretreatment methods for the sugar recovery and structural changes. Bioresour. Technol. 129, 592–598.
Zhang, Y.P., Lynd, L.R., 2004. Toward an aggregated understanding of enzymatic hydrolysis of cellulose: noncomplexed cellulase systems. Biotechnol. Bioeng. 88 (7), 797–824. http://dx.doi.org/10.1002/bit.20282.